Neuronal avalanches in Watts-Strogatz networks of stochastic spiking neurons

Renata Pazzini,[1] Osame Kinouchi,[1] and Ariadne A. Costa[2,*]
[1]*Universidade de São Paulo, FFCLRP, Departamento de Física, Ribeirão Preto, São Paulo 14040-901, Brazil*
[2]*Grupo de Redes Complexas Aplicadas de Jataí, Universidade Federal de Jataí, Jataí, GO 75801-615, Brazil*

(Received 7 June 2021; accepted 8 June 2021; published 26 July 2021)

Networks of stochastic leaky integrate-and-fire neurons, both at the mean-field level and in square lattices, present a continuous absorbing phase transition with power-law neuronal avalanches at the critical point. Here we complement these results showing that small-world Watts-Strogatz networks have mean-field critical exponents for any rewiring probability $p > 0$. For the ring ($p = 0$), the exponents are the same from the dimension $d = 1$ of the directed-percolation class. In the model, firings are stochastic and occur in discrete time steps, based on a sigmoidal firing probability function. Each neuron has a membrane potential that integrates the signals received from its neighbors. The membrane potentials are subject to a leakage parameter. We study topologies with a varied number of neuron connections and different values of the leakage parameter. Results indicate that the dynamic range is larger for $p = 0$. We also study a homeostatic synaptic depression mechanism to self-organize the network towards the critical region. These stochastic oscillations are characteristic of the so-called self-organized quasicriticality.

DOI: 10.1103/PhysRevE.104.014137

I. INTRODUCTION

Criticality in the brain is a vastly reported phenomenon [1–3]. It implies that the networks of neurons can produce avalanches of spikes with both size and duration distributed according to power laws. The operation near a critical state has been presented as a sign of brain health [4,5], besides optimization of information transmission and storage, metastable states, computational power, and dynamic range, as revealed by experiments and modeling [6–15].

Although the leaky integrate and fire (LIF) model is one of the most studied models for simulating neural systems [16], experiments have shown that cortical neurons respond reliably to time-dependent input, with small trial-to-trial variations if the same stimulus is repeated [17,18]. That is a motivation for using stochastic LIF models.

Discrete-time stochastic neurons have a history since the 1980s (Boltzman machines, Hopfield networks with stochastic neurons). In 1992, Gerstner and van Hemmen introduced a discrete time stochastic spiking neuron model [19], which is very similar to the model used here, with a different (exponential) spike probability function. This model is also discussed in a well-known book [20]. After that, several groups have been studying stochastic neurons [21–26].

Systems belonging to the same *universality class* share the same behavior near the critical point, particularly the critical exponents [27,28]. One may group even very different systems into a reduced number of universality classes due to similarities at the microscopic level. Recently, it has been shown that a class of the stochastic LIF neurons present a continuous absorbing phase transition in the directed percolation (DP) universality class [24,29]. Such transition is typical of self-organized critical models (SOCs) and it has been used to explain neuronal avalanche experiments [1,9,30,31].

An important question refers to the mechanism that could tune the networks to the critical region. In a seminal paper, Levina, Hermann, and Geisel (LHG) [32] proposed depressing and recovering synapses as such a mechanism. The LHG model was analyzed in depth by Bonachela *et al.* [33]. They found that the achieved state is not true SOC: The system hovers around the critical point with stochastic oscillations, which has been called self-organized quasicriticality or SOqC. Indeed, this is typical for any nonconservative system like earthquake, forest fire, and neuronal network models [34].

It also has been shown that other biologically plausible mechanisms (dynamic neuronal gains [26,29] and adaptive firing thresholds [35]) can lead to SOqC. In all these studies, however, all-to-all (complete graph) networks have been used. The motivation for that was to compare results with mean-field calculations. However, this topology is not biologically realistic. Also, complete graphs present problems for computational simulation of dynamic synapses, since a network with N neurons has $N(N-1)$ synaptic equations, preventing the work with large systems.

In this respect, random networks are a bit more realistic and computationally tractable. Indeed, random networks of stochastic cellular automata with dynamic synapses have been studied [36,37]. However, such cellular automata do not have important biological features of integrate-and-fire neurons, like a continuous state variable (membrane potential), a leakage parameter, or a firing threshold.

In this work, we use networks one step further in terms of complexity: The Watts-Strogatz (WS) graphs [38]. This topology combines both short- and long-range connections, presenting a small average shortest path length and a large

*Corresponding author: ariadne.costa@ufj.edu.br

clustering coefficient. Indeed, these features are recognized properties that mimic biological neuronal networks [39–42]. Here, we study phase transitions and critical avalanches in WS networks of stochastic discrete-time leaky integrate-and-fire neurons. The parameters varied are the probability of rewiring p, the leakage parameter μ, and the number of neighbors K. We also report preliminary results of a homeostatic mechanism that lead to SOqC in WS networks.

II. METHODS

Our system is a network of discrete-time stochastic integrate-and-fire neurons. The network follows the WS topology [38], constructed using the package NETWORKX for Python. The function creates a ring over N neurons, and each one is connected with its K nearest neighbors (we assume even values for K). Then shortcuts are created by replacing some edges in the follow way: For each connection of the ring, with probability p, replace it with a new connection i-j with a uniformly random choice of an existing neuron j.

The membrane potential of a neuron i ($i = 1, \ldots, N$) evolves as

$$V_i[t+1] = \mu_i V_i[t] + I_i[t] + \frac{1}{k_i}\sum_{j=1}^{k_i} W_{ij} X_j[t]\,, \tag{1}$$

where μ is the leakage parameter, $I_i[t]$ is an external input, and k_i is the number of connections for neuron i. Notice the neurons can have a different number of connections after rewiring. The element W_{ij} gives the synaptic weight between the jth presynaptic neuron and the ith postsynaptic neuron ($W_{ij} = 0$ if the neurons are not connected). The jth presynaptic neuron can be any site $j \in \{1, ..., N\}$ with $j \neq i$.

If at a time step t the neuron fires, its membrane potential is reset as $V_i[t+1] = 0$; otherwise, the neuron follows Eq. (1). The stochastic firing is implemented as

$$P(X_i[t] = 1 \mid V_i[t]) \equiv \Phi(V_i[t])\,, \tag{2}$$

in which $\Phi(V)$ is the firing function that governs the probability of a neuron to emit an action potential. The model incorporates an absolute refractory period of one time step by imposing $\Phi(0) = 0$. In principle, any sigmoidal $\Phi(V)$ function works, but for convenience we use the so called rational function [26,29]:

$$\Phi_i(V) = \frac{\Gamma_i(V_i - \theta_i)}{1 + \Gamma_i(V_i - \theta_i)}\,\Theta(V_i - \theta_i), \tag{3}$$

where $\Theta(x)$ is the Heaviside step function. Here, θ_i is a firing threshold value of the membrane potential, below which the neuron cannot fire, i.e., $\Phi(V_i) = 0$ for $V_i < \theta_i$. The Γ_i in Eq. (3) is the neuronal gain. The firing threshold is a parameter experimentally related to the phenomenon of firing rate adaptation [43–45]. Notice the limit $\Phi(V) \to 1$ for large V, as it should be for a well-behaved probability function.

The activity of a system with N neurons is, at any time step,

$$\rho[t] = \langle X_i[t]\rangle \equiv \frac{1}{N}\sum_{i=1}^{N} X_i[t]\,, \tag{4}$$

where $\langle \ldots \rangle$ is the average over sites. A control parameter for this model is the average synaptic weight $W = \langle W_{ij}\rangle$. We assume here that the distribution $P(W_{ij})$ has finite variance and well-defined average. The same is assumed for the leakage parameters μ_i, gains Γ_i, inputs I_i, and firing thresholds θ_i, so that $\mu = \langle \mu_i\rangle$, $\Gamma = \langle \Gamma_i\rangle$, $I = \langle I_i[t]\rangle$, and $\theta = \langle \theta_i\rangle$ can be also considered as control parameters.

Discarding a transient period t_t, the time-averaged network activity is

$$\rho = \langle \rho[t]\rangle_t \equiv \frac{1}{t_f - t_t}\sum_{t=t_t}^{t_f} \rho[t]\,, \tag{5}$$

where t_f is a large time period. We assume that, given constant parameters I, μ, θ, Γ, and W, there is a stationary activity (fixed point) $\rho(W|\Gamma, I, \mu, \theta)$. This activity or firing density is our order parameter.

However, the closer to the probability $p = 1$ for the WS topology, the closer to an Erdös and Rényi network, which in the limit $K = N - 1 \to \infty$ corresponds to the mean-field case [46,47]. In this sense, we can gain insight by calculating ρ as [24]

$$\rho[t+1] = \int \Phi(V) P(V)[t]\, dV\,, \tag{6}$$

where $P(V)[t]$ is the distribution of membrane potentials at time t. If $\mu > 0$, there is an efficient numerical method to calculate this integral [24,26,29]. However, for $\mu = 0$, a very simple analytic solution is available because the potential density corresponds to only two Dirac peaks, $P(V)[t] = \rho\delta(V) + (1-\rho)\delta(V - W\rho[t] - I)$. Together with Eq. (3), this leads to the mean-field map:

$$\rho[t+1] = \frac{(W\rho[t] + h)(1 - \rho[t])\Gamma}{1 + (W\rho[t] + h)\Gamma}\,\Theta(W\rho + h)\,, \tag{7}$$

where $h = I - \theta$ is the suprathreshold current.

Studying the stationary states of Eq. (7) we see that the system presents a continuous phase transition for $h = 0$ [26,29,35]. When the field is $h < 0$ we have a first order phase transition, and when $h > 0$ there is no transition. Here, to set $h = 0$ seems to be less natural than to set zero magnetic field for spin systems because I and θ must be fine tuned. Later we discuss how a self-organizing mechanism for $\theta_i[t]$ (adaptive firing thresholds) can tune h toward zero in average. By now, we assume $h = 0$ and study the continuous phase transition.

III. RESULTS

A. Phase transitions

In statistical physics, we usually have two versions of a model to study: quenched and annealed. In the quenched case, the network is randomly created just once at the beginning and is kept throughout the simulation; case annealed, on the other hand, implies a new random definition of the network each time step. Although the quenched case is more realistic, the annealed one is often studied because it is more comparable to theoretical mean-field calculations [37,48].

We first show a comparison of quenched and annealed cases for the dependence of ρ on W for different values of rewiring probabilities p in Fig. 1. In the Watts-Strogatz

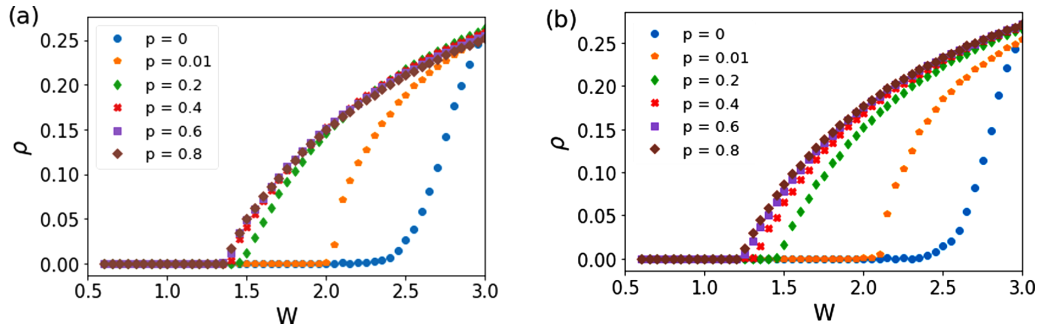

FIG. 1. (a) Quenched and (b) annealed phase transitions of $\rho(W|p)$ for several rewiring probabilities p. Parameters $K = 4$ and $N = 10\,000$.

topology, one observes a continuous absorbing-state phase transition if $h = 0$. Close to the critical point $W_c(p)$, for $\mu = 0$, we have

$$\rho(W|p) = C(p)\left(\frac{W - W_c(p)}{W}\right)^{\beta}. \tag{8}$$

Figure 1 shows no qualitative differences between quenched and annealed. The quantitative differences of the respective critical points vary from 0 to 9.5% in the figure. These differences are coherent, increasing for larger p. When $p = 0$ we have always the same network (the ring) in both quenched and annealed cases. The more long-range interactions, the larger the difference between the critical points. For Erdös and Rényi networks (equivalent to $p = 1$ WS topology), approximately 10% of variation has already been found for the two cases applied to another neuron network model [37]. These variations can be carefully studied in a future work. So, from now on, the figures correspond to the annealed case, given the similarity to mean-field calculations.

In the mean-field case, when $h = 0$ the stationary map of Eq. (7) (in which $\rho[t+1] = \rho[t] = \rho$) provides

$$\rho(W, \Gamma) = \frac{1}{2}\left(\frac{W - W_c(\Gamma)}{W}\right), \tag{9}$$

$$W_c(\Gamma) = 1/\Gamma\,, \tag{10}$$

where $\rho = 0$ (absorbing state) for $W < W_c$. The hyperbolae $W_c(\Gamma)$ is a critical line in the plane $W \times \Gamma$, but we can absorb the variables Γ, W into a single one, i.e., $\overline{W} = \Gamma W$. Absorbing the gain parameter Γ in W is equivalent to setting $\Gamma = 1$, without loss of generality. So, we fix $\Gamma = 1$, which means $W = \overline{W}$.

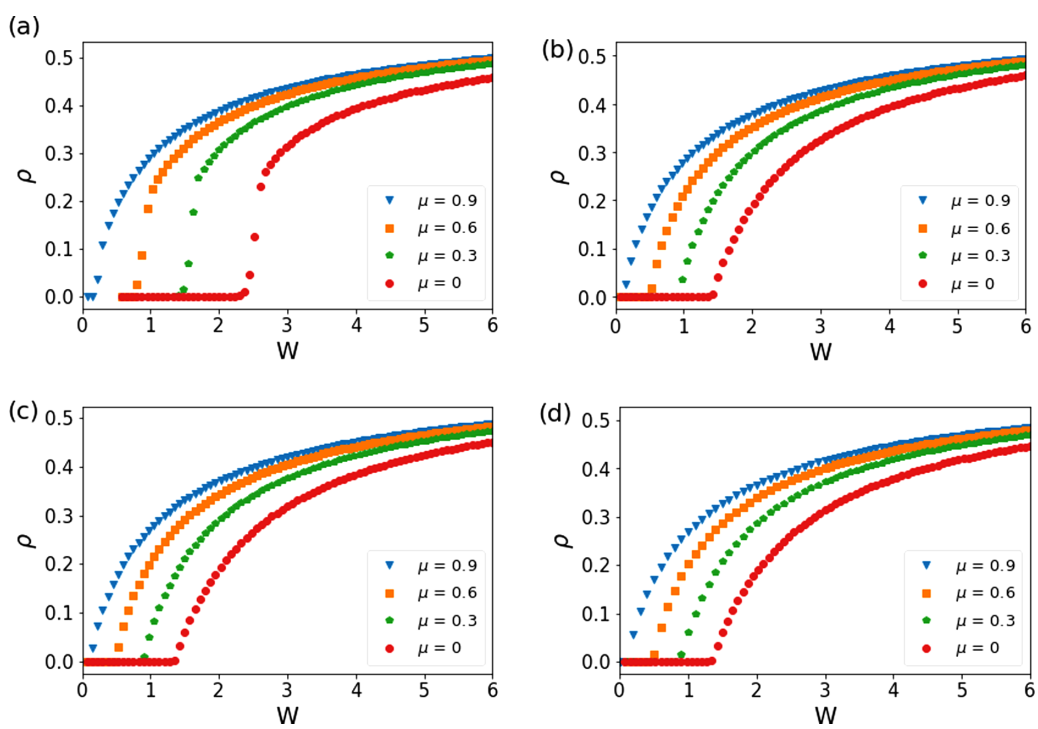

FIG. 2. Curves $\rho(W|\mu)$ for several values of the rewiring probability p with $K = 4$ and $N = 10\,000$. (a) $p = 0$, (b) $p = 0.3$, (c) $p = 0.6$, (d) $p = 1.0$.

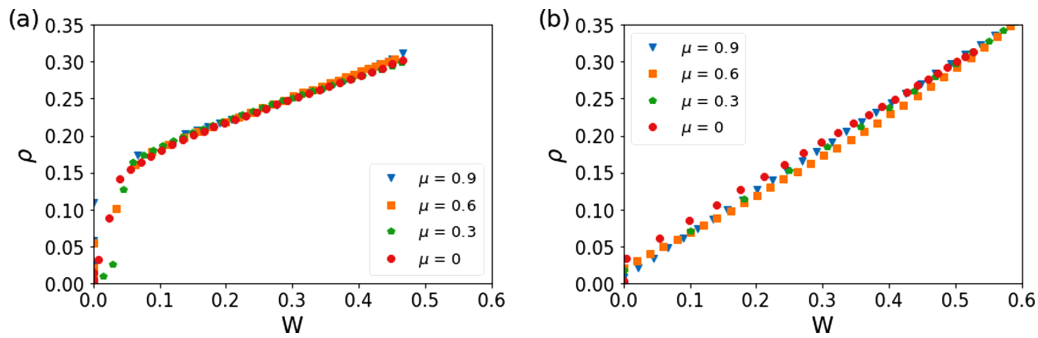

FIG. 3. Collapse of $\rho(W|\mu)$ for (a) $p = 0.0$ and (b) $p = 1.0$. $N = 10\,000$ and $K = 4$.

Recently it has been found for a square lattice of stochastic neurons [49]

$$\rho(W|\mu) = C(\mu)\left(\frac{W - W_c(\mu)}{W}\right)^{\beta}, \tag{11}$$

with dimension $d = 2$ DP exponent $\beta = 0.583$. Here we have similar results for $\rho(W|\mu, p)$ (Fig. 2), but with $\beta = 1$ for $p > 0$ and $\beta = 0.276$ for $p = 0$, as one might expect [50,51]. We find the exponents by applying the data collapse $\rho(x) = \frac{1}{2}x$ with $x = (W - W_c)/W$ in Eq. (8); see Fig. 3. In general, the collapse means that a system or function is the same if the scales of length, energy, or other variables are multiplied by a common factor (i.e., if they are rescaled). It represents universality. This property, also found in studies of the brain [52,53], is called *scale invariance*.

The results suggest that any fraction (>0) of long-range links makes the network behave as a mean-field one, irrespective of the clustering coefficient of the WS topology. We see that it is possible to generalize it including the dependence not only on μ but also for K and p, i.e., $\rho(\mu, K, p)$. The form is

$$\rho(W|p, \mu, K) = C(p, \mu, K)\left(\frac{W - W_c(p, \mu, K)}{W}\right)^{\beta}; \tag{12}$$

see Figs. 4 and 5.

It means that, in principle, we can obtain total data collapse, showing that the parameters p, μ, K do not change the universality class of the transition (directed percolation) and only the case $p = 0$ ($d = 1$) affects the value of the critical exponent.

At the mean-field level, it is possible to calculate the prefactor $C(\mu)$ for moderate μ, exact to $\mathcal{O}(\mu^2)$ [29]:

$$C(\mu) = \frac{1}{2 + \mu + \mu^2/(1 - \mu)}. \tag{13}$$

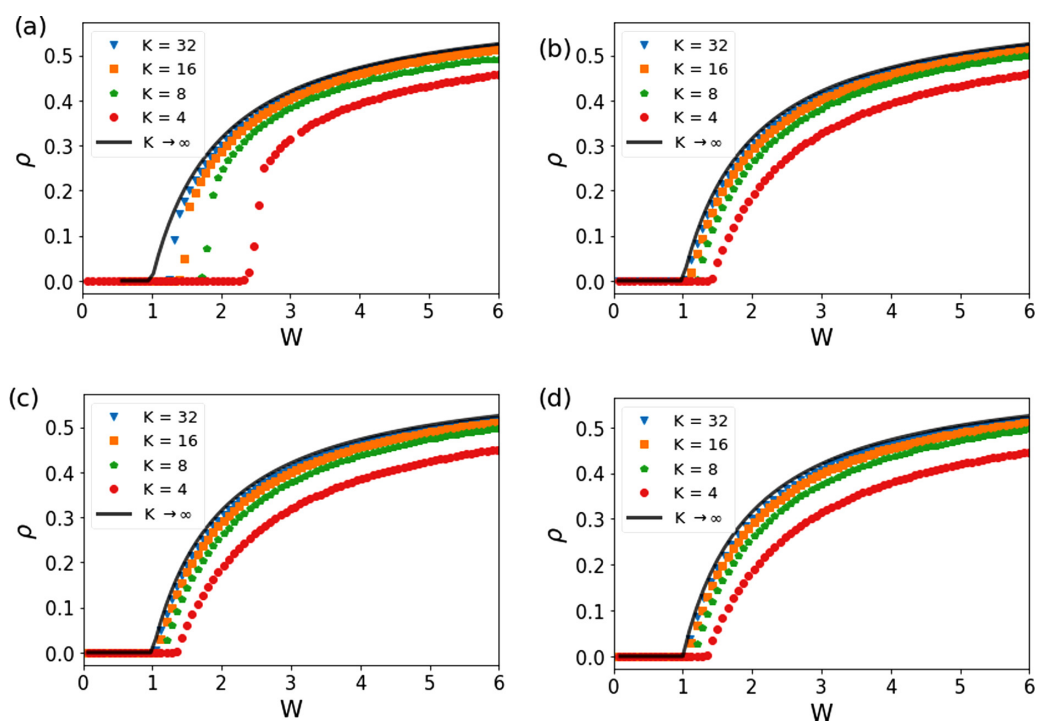

FIG. 4. Curves $\rho(W|K)$ for several values of p with $\mu = 0$ and $N = 10\,000$. (a) $p = 0$, (b) $p = 0.3$, (c) $p = 0.6$, (d) $p = 1.0$.

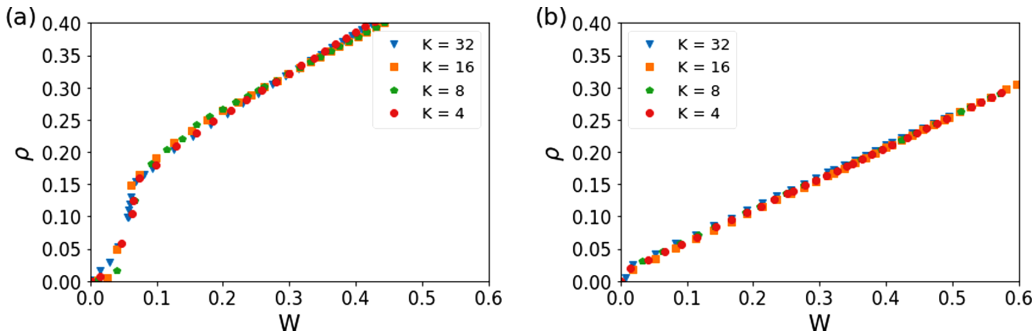

FIG. 5. Collapse of $\rho(W|K)$ for (a) $p = 0.0$ and (b) $p = 1.0$ with $N = 10\,000$ and $\mu = 0$.

B. Neuronal avalanches

In the Watts-Strogatz topology we have two types of neuronal avalanches: those with $p = 0$ ($d = 1$) and those with $p > 0$ (mean-field like with long range connections). To extract the avalanche critical exponents from our integrate-and-fire stochastic network, we made a finite size study of avalanche size and duration.

As a function of N, we calculate the avalanche size complementary cumulative distribution function:

$$F(s) = \sum_{x=s}^{\infty} P_s(x)\,; \tag{14}$$

see Fig. 6. We expect a power law $F(s) \propto s^{1-\tau}$ since the avalanche size distribution is $P_s(x) \propto x^{-\tau}$.

We also see a clear N-dependent finite size cutoff. So, we scale the horizontal axis as s/N^c and the vertical axis as $F(s)s^{\tau-1}$ (Fig. 7). Data collapse leads to a cutoff exponent $c = 1$, and avalanche exponents $\tau = 1.11$ for $p = 0$ and $\tau = 1.5$ for $p > 0$. They are compatible with the $d = 1$ DP avalanche exponent $\tau = 1.108$ and the mean-field result $\tau = 3/2$, respectively (see Table I).

We do the same for avalanche durations (d). The complementary cumulative distribution function is

$$F(d) = \sum_{x=d}^{\infty} P_d(x)\,, \tag{15}$$

presented in Fig. 8. We expect a power law $F(d) \propto s^{1-\tau_d}$ since $P_d(x) \propto d^{-\tau_d}$. The collapsed data (Fig. 9) give $c = 1/2$, $\tau_d = 1.16$ for $p = 0$ and $\tau_d = 2$ for $p > 0$, which is also compatible with the $d = 1$ DP value $\tau_d = 1.159$ and the mean-field value $\tau_d = 2$; see Table I.

The case $p = 0$ has only technical interest, since the exponents observed experimentally never correspond to $d = 1$ but to mean-field DP [54]. For $p > 0$, due to the presence of long-range links, all results obtained are compatible with the statistics of mean-field DP, the usual result for neuronal avalanches [1,24,35–37,50,55–58]. In other words,

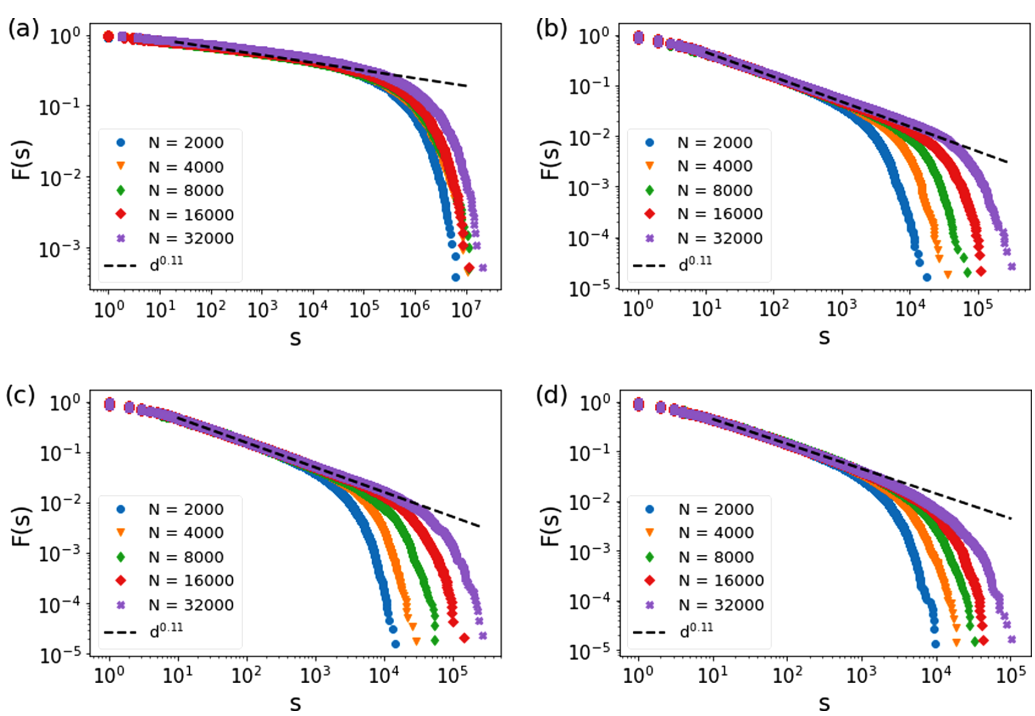

FIG. 6. Avalanche size distribution $F(s)$ for several values of N. Leakage $\mu = 0$ and $K = 4$. (a) $p = 0$, (b) $p = 0.3$, (c) $p = 0.6$, (d) $p = 1.0$.

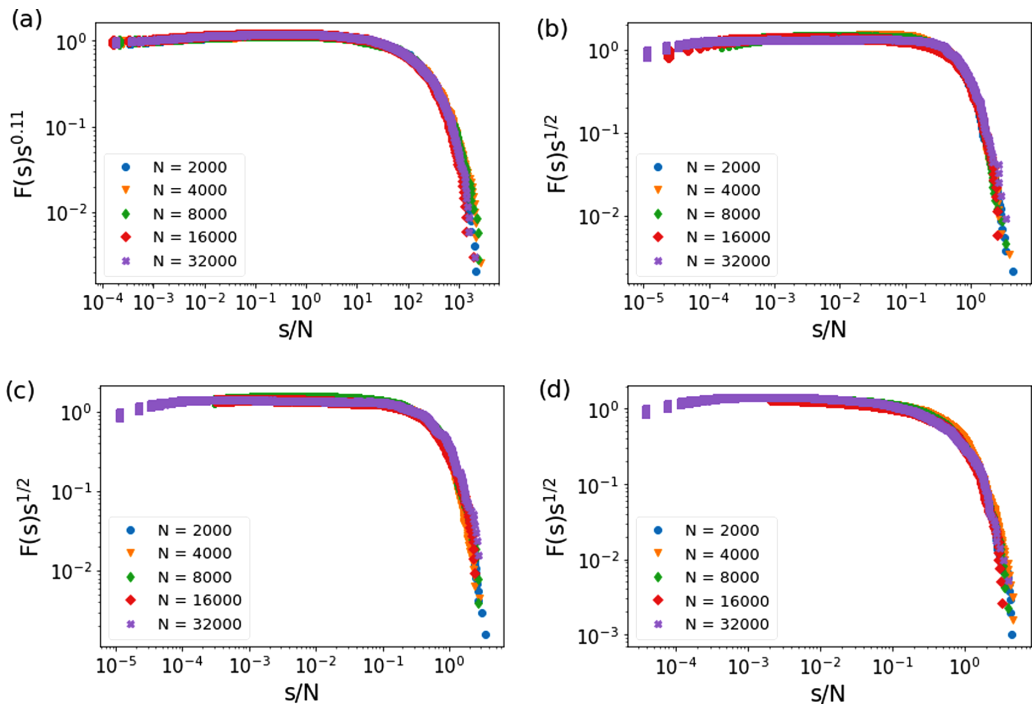

FIG. 7. Data collapse of the avalanches presented in Fig. 6. (a) $p = 0$, (b) $p = 0.3$, (c) $p = 0.6$, (d) $p = 1.0$.

even if WS graphs really describe neuronal networks, the experimental data are unable to constrain the random link fraction p. Indeed, any complex network model such as Erdös-Renyi, scale-free Barabasi-Albert, hierarquical models, etc., is subdetermined by the mean-field-like exponents found in experiments [59].

C. Self-organized quasicriticality

We now propose a homeostatic mechanism to tune the system around the critical region (self-organized quasicriticality or SOqC [24,26,29,33–35,59]). In this sense, we introduce depressing-recovering synapses in a simplified way (we call it the constant drive model [59]):

$$W_{ij}[t+1] = W_{ij}[t] + \frac{1}{\tau_w} - uW_{ij}[t]X_j[t]\,, \qquad (16)$$

where we remember that the synaptic weight average is $W[t] \equiv \langle W_{ij}[t]\rangle$.

This synaptic mechanism has a recovery time τ_w and a synaptic depressing fraction $0 < u < 1$. Note that this dynamics is simpler than the LHG one [32,33].

TABLE I. Order parameter critical exponent β and avalanche exponents τ and τ_d. The case $p = 0$ corresponds to $d = 1$ and for $p > 0$ we find mean-field values [50].

Exponent	$d = 1$	$d = 2$	$d = 3$	MF
β	0.276	0.583	0.805	1
τ	1.108	1.268	1.395	3/2
τ_d	1.159	1.450	1.730	2

The fixed point condition of Eq. (17) is

$$W^*\rho^* = \frac{1}{\tau_w u}\,, \qquad (17)$$

Now we make a mean-field calculation, valid for complete graphs, which gives some intuition for the WS case. We also have the quasicritical activity $\rho^* = \mathcal{O}[1/(\tau_w u)] \approx 0$. For any initial conditions, after a transient, the coordinates $(W[t])$ finally hover around the quasicritical fixed point (W^*), characterizing a SOqC system. The same happens for different τ_w values.

We remember that the above mean-field calculations are valid for an infinite complete graph and are reported here only to give some intuition about the self-organization process in the model. We reserve a full study of the homeostatic dynamics for a future paper. Here we only give preliminary results for a WS network with $p = 0.6$, $\mu = 0$, $I = 0$, $K = 4$, $u = 0.1$, and $N = 10\,000$; see Fig. 10.

In this self-organized quasicritical system we have a fixed point focus that loses stability for $\tau_w \to \infty$. This focus, perturbed by finite-size (demographic) noise, creates the stochastic oscillations which, however, have decreasing amplitude as a function of N [26]. Regardless, if noise is environmental, which is more realistic in terms of biology, it does not decrease with N and stochastic oscillations would be always present (to be studied deeply in a future work). Interestingly, with our time step $\delta t = 1$ ms, the quasiperiodic oscillations lie in the range δ-γ EEG brain waves, the frequency being controlled by the recovery time τ_w [29].

IV. DISCUSSION

The order parameter behaves as $\rho(W = W_c, h) \propto h^{1/\delta_h}$, where δ_h is the field critical exponent [35]. Here, h is the

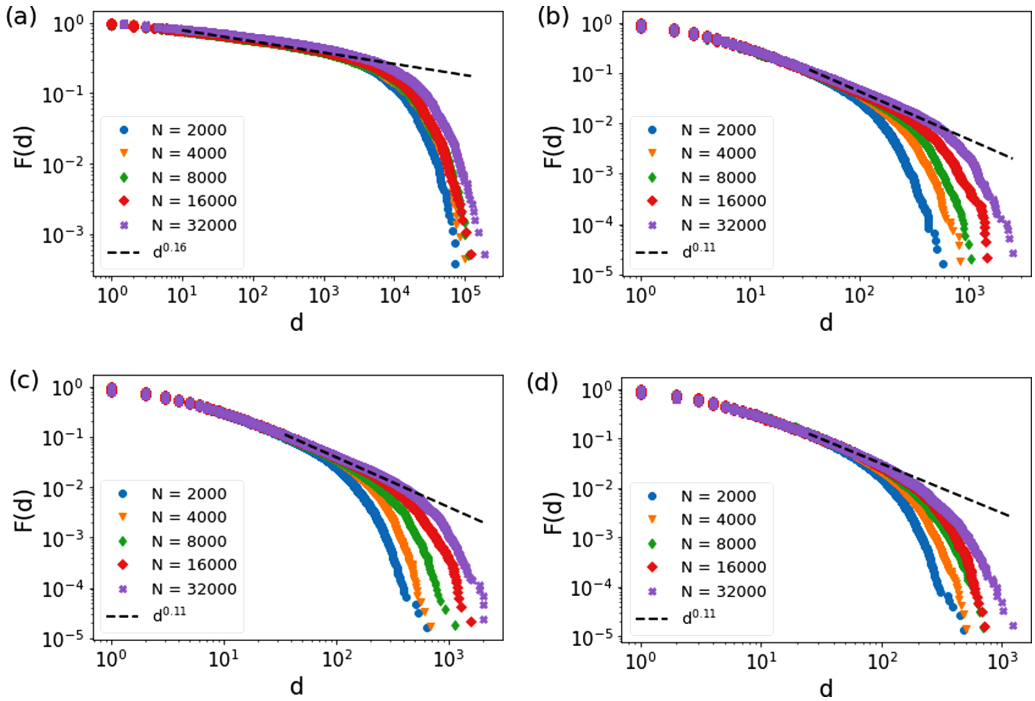

FIG. 8. Avalanche duration distribution $F(d)$ for several values of N. (a) $p = 0$, (b) $p = 0.3$, (c) $p = 0.6$, (d) $p = 1.0$. Leakage $\mu = 0$ and $K = 4$.

previously defined field $h = I - (1 - \mu)\theta$ (for $\mu = 0$ this is the suprathreshold current). This means that the network response has a very large dynamic range at criticality; because of the so called Stevens's psychophysical exponent $m = 1/\delta_h$ is small and $\rho(h)$ is a very compressing function [8,48,49,60–62]. On the other hand, out of the critical point, we have a linear relation $\rho(h) \propto h$ and the network mapping between the input h and the network output $\rho(h)$ is very limited [8,49].

When $p > 0$, we have the mean-field value $\delta_h = 2$ so that the compressing exponent is $m = 1/2$ [8]. This means that, say, an $\mathcal{O}(10^2)$ order of magnitude input h can be mapped to an $\mathcal{O}(10)$ output activity ρ. More interestingly, for the ring

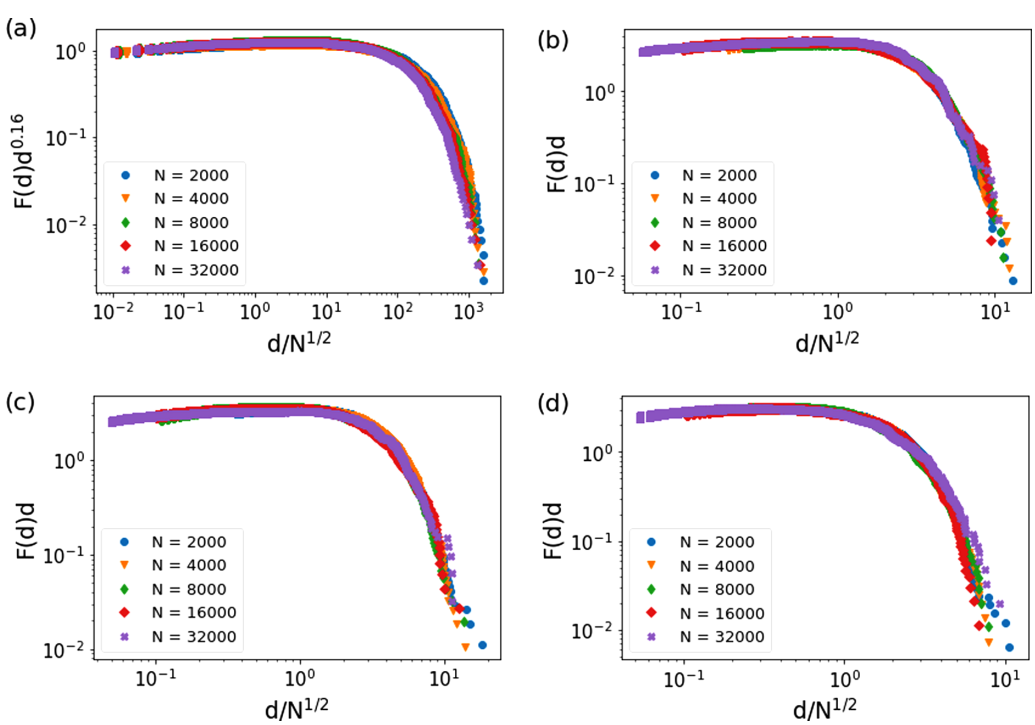

FIG. 9. Data collapse: avalanche duration distribution $F(d)$ for (a) $p = 0$, (b) $p = 0.3$, (c) $p = 0.6$, (d) $p = 1.0$. Leakage $\mu = 0$ and $K = 4$.

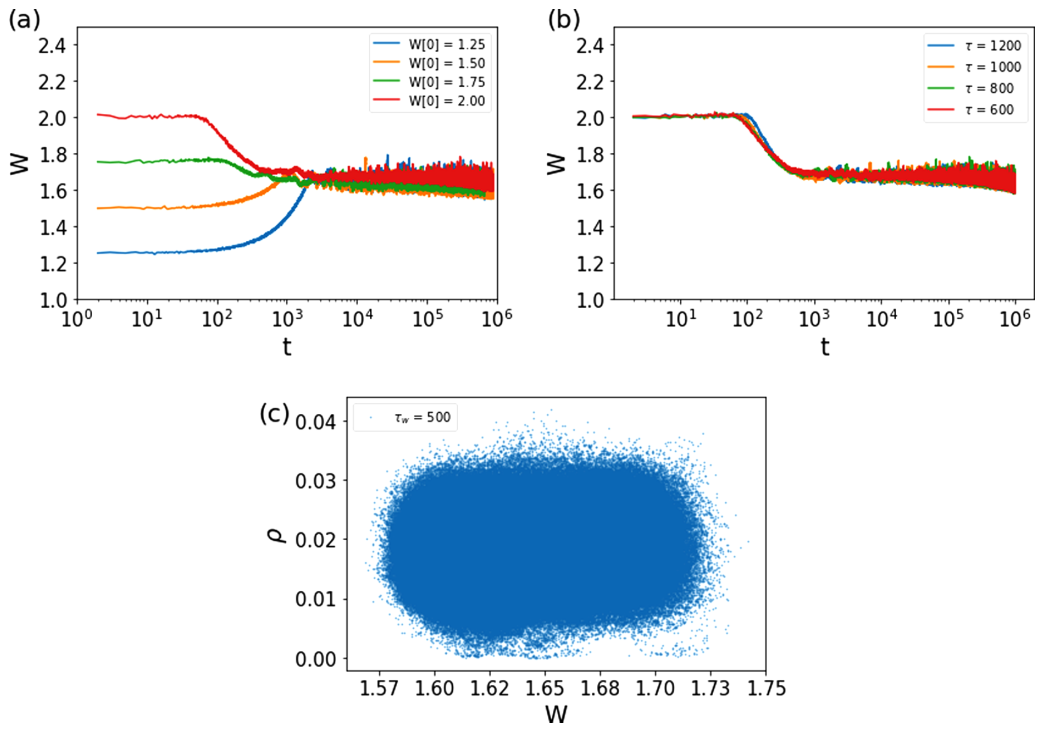

FIG. 10. Time series of the homeostatic variables for (a) $W[t]$ for several initial conditions $W[0]$ (with $\tau_w = 800$); (b) $W[t]$ for several τ_w; (c) trajectory of the homeostatic system in the plane ρ vs W. Parameters: $p = 0.6$, $\mu = 0$, $I = 0$, $K = 4$, $u = 0.1$, and $N = 10\,000$.

of neurons ($p = 0$), we have the DP value $m = 1/\delta_h = 0.111$ [50,51], which means that an $\mathcal{O}(10^9)$ signal can be compressed to an $\mathcal{O}(10)$ output. This extreme performance seems to be excessive even for biological sensors: The difference between luminosity at noon and at moonlight is about 10^{12} and this dynamic range is dealed by the human eye with several complementary systems, including adaptive firing rates. However, it could be interesting to search if other biological or artificial $d = 1$ sensors, based in excitable elements, could achieve this performance.

One suggestion could be that linear sensory organs, like the lateral line system of fishes [63,64], could be tuned to criticality to optimize their dynamic range. By now, this is only a conjecture for a future work. Anyway, artificial sensors with this principle [8,65,66] could be constructed.

V. CONCLUSION

The case $p = 0$ (large world) corresponds to a one-dimensional system and presents the corresponding $d = 1$ DP critical exponents. In this case, avalanches are very large when compared to N, meaning not only that finite size effects are important but also that the same neuron participates of the avalanche several times, in contrast with avalanches for $p > 0$.

If we include the small-world shortcuts ($p > 0$), we have networks that present mean-field exponents compatible with neuronal avalanche experiments. It is worth mentioning we considered only sparse networks ($K \ll N$) and the phase transition also depends on the leakage parameter μ, that is, $W_c = W_c(p, K, \mu)$. Anyway, we have showed that full data collapse can be achieved if we use $\rho(x)$ with the variable $x = [W - W_c(p, K, \mu)]/W$.

In the context of SOqC, we are aware of only two studied topologies: random networks of cellular automata with K neighbors [36,37] and complete graphs of continuous-time LIF neurons [32,33] or discrete-time stochastic LIF neurons [24,26,29,35,67]. Hence, our examination of SOqC behavior in the Watts-Strogatz topology is a welcome addition to this literature.

As a future work, we intend to make extensive simulations on homeostatic mechanisms to verify their stability and the dependence on N for the stochastic oscillation amplitude caused by environmental noise [26]. Finally, it is possible to characterize the frequency spectrum of the stochastic oscillations, applying this to the modeling of brain waves.

ACKNOWLEDGMENTS

R.P. thanks CAPES for the scholarship #88882.378804/2019-01. A.A.C. and R.P. thanks FAPEG (Grant No. 17833-03/2015) and P. F. Gomes. O.K. acknowledges CNAIPS-USP support and FAPESP Scholarship BPE No. 2019/12746-3. This article was produced as part of the activities of FAPESP Research, Innovation and Dissemination Center for Neuromathematics (Grant No. 2013/07699-0, S. Paulo Research Foundation). The present research also had the support of CNPq, Conselho Nacional de Desenvolvimento Científico e Tecnológico, Brazil.

[1] J. M. Beggs and D. Plenz, J. Neurosci. **23**, 11167 (2003).
[2] J. M. Beggs and D. Plenz, J. Neurosci. **24**, 5216 (2004).
[3] L. De Arcangelis, F. Lombardi, and H. Herrmann, J. Stat. Mech.: Theory Exp. (2014) P03026.

[4] L. Cocchi, L. L. Gollo, A. Zalesky, and M. Breakspear, Prog. Neurobiol. (Oxford, U. K.) **158**, 132 (2017).
[5] V. Zimmern, Front. Neural Circuits **14**, 54 (2020).
[6] W. Maass, T. Natschläger, and H. Markram, Neural Comput. **14**, 2531 (2002).
[7] C. Haldeman and J. M. Beggs, Phys. Rev. Lett. **94**, 058101 (2005).
[8] O. Kinouchi and M. Copelli, Nat. Phys. **2**, 348 (2006).
[9] J. M. Beggs, Philos. Trans. R. Soc. A **366**, 329 (2008).
[10] T. Tanaka, T. Kaneko, and T. Aoyagi, Neural Comput. **21**, 1038 (2009).
[11] J. Boedecker, O. Obst, J. T. Lizier, N. M. Mayer, and M. Asada, Theory Biosci. **131**, 205 (2012).
[12] W. L. Shew and D. Plenz, Neuroscientist **19**, 88 (2013).
[13] S. H. Gautam, T. T. Hoang, K. McClanahan, S. K. Grady, and W. L. Shew, PLoS Comput. Biol. **11**, e1004576 (2015).
[14] O. Shriki and D. Yellin, PLoS Comput. Biol. **12**, e1004698 (2016).
[15] H. Hoffmann and D. W. Payton, Sci. Rep. **8**, 2358 (2018).
[16] A. N. Burkitt, Biol. Cybern. **95**, 1 (2006).
[17] H. L. Bryant and J. P. Segundo, J. Physiol. **260**, 279 (1976).
[18] Z. F. Mainen and T. J. Sejnowski, Science **268**, 1503 (1995).
[19] W. Gerstner and J. L. van Hemmen, Netw. Comput. Neural Syst. **3**, 139 (1992).
[20] W. Gerstner and W. M. Kistler, *Spiking Neuron Models: Single Neurons, Populations, Plasticity* (Cambridge University Press, Cambridge, UK, 2002).
[21] N. Kasabov, Neural Networks **23**, 16 (2010).
[22] A. Galves and E. Löcherbach, J. Stat. Phys. **151**, 896 (2013).
[23] D. B. Larremore, W. L. Shew, E. Ott, F. Sorrentino, and J. G. Restrepo, Phys. Rev. Lett. **112**, 138103 (2014).
[24] L. Brochini, A. A. Costa, M. Abadi, A. C. Roque, J. Stolfi, and O. Kinouchi, Sci. Rep. **6**, 35831 (2016).
[25] P. E. Greenwood and L. M. Ward, *Stochastic Neuron Models* (Springer, New York, Cham, Switzerland, 2016), Vol. 1.
[26] O. Kinouchi, L. Brochini, A. A. Costa, J. G. F. Campos, and M. Copelli, Sci. Rep. **9**, 3874 (2019).
[27] M. Plischke and B. Bergersen, *Equilibrium Statistical Physics* (World Scientific, Singapore, 1994).
[28] S.-K. Ma, *Modern Theory of Critical Phenomena* (Routledge, New York, 2018).
[29] A. A. Costa, L. Brochini, and O. Kinouchi, Entropy **19**, 399 (2017).
[30] D. R. Chialvo, Nat. Phys. **6**, 744 (2010).
[31] M. A. Muñoz, Rev. Mod. Phys. **90**, 031001 (2018).
[32] A. Levina, J. M. Herrmann, and T. Geisel, Nat. Phys. **3**, 857 (2007).
[33] J. A. Bonachela, S. de Franciscis, J. J. Torres, and M. A. Muñoz, J. Stat. Mech. (2010) P02015.
[34] J. A. Bonachela and M. A. Muñoz, J. Stat. Mech. (2009) P09009.
[35] M. Girardi-Schappo, L. Brochini, A. A. Costa, T. T. A. Carvalho, and O. Kinouchi, Phys. Rev. Research **2**, 012042(R) (2020).
[36] A. A. Costa, M. Copelli, and O. Kinouchi, J. Stat. Mech. (2015) P06004.
[37] J. G. F. Campos, A. A. Costa, M. Copelli, and O. Kinouchi, Phys. Rev. E **95**, 042303 (2017).
[38] D. J. Watts and S. H. Strogatz, Nature (London) **393**, 440 (1998).
[39] O. Shefi, I. Golding, R. Segev, E. Ben-Jacob, and A. Ayali, Phys. Rev. E **66**, 021905 (2002).
[40] M. D. Humphries, K. Gurney, and T. J. Prescott, Proc. R. Soc. B: Biol. Sci. **273**, 503 (2006).
[41] J. H. Downes, M. W. Hammond, D. Xydas, M. C. Spencer, V. M. Becerra, K. Warwick, B. J. Whalley, and S. J. Nasuto, PLoS Comput. Biol. **8**, e1002522 (2012).
[42] D. S. Bassett and E. T. Bullmore, Neuroscientist **23**, 499 (2017).
[43] B. Ermentrout, M. Pascal, and B. Gutkin, Neural Comput. **13**, 1285 (2001).
[44] J. Benda and A. V. M. Herz, Neural Comput. **15**, 2523 (2003).
[45] A. Buonocore, L. Caputo, E. Pirozzi, and M. F. Carfora, Math. Biosci. Eng. **13**, 483 (2016).
[46] B. Bollobás, *Random Graphs* (Cambridge University Press, Cambridge, UK, 2001), Vol. 73.
[47] R. Cohen and S. Havlin, *Complex Networks: Structure, Robustness and Function* (Cambridge University Press, Cambridge, UK, 2010).
[48] D. B. Larremore, W. L. Shew, and J. G. Restrepo, Phys. Rev. Lett. **106**, 058101 (2011).
[49] E. F. Galera and O. Kinouchi, Phys. Rev. Research **2**, 033057 (2020).
[50] M. A. Munoz, R. Dickman, A. Vespignani, and S. Zapperi, Phys. Rev. E **59**, 6175 (1999).
[51] S. Lübeck, Int. J. Mod. Phys. B **18**, 3977 (2004).
[52] P. Gong, A. R. Nikolaev, and C. Van Leeuwen, Neurosci. Lett. **336**, 33 (2003).
[53] B. J. He, Trends Cognit. Sci. **18**, 480 (2014).
[54] T. T. Carvalho, A. J. Fontenele, M. Girardi-Schappo, T. Feliciano, L. A. Aguiar, T. P. Silva, N. A. de Vasconcelos, P. V. Carelli, and M. Copelli, Front. Neural Circuits **14**, 83 (2021).
[55] H. J. Jensen, *Self-organized Criticality: Emergent Complex Behavior in Physical and Biological Systems* (Cambridge University Press, Cambridge, UK, 1998).
[56] R. Dickman, M. A. Muñoz, A. Vespignani, and S. Zapperi, Braz. J. Phys. **30**, 27 (2000).
[57] G. Pruessner, *Self-organised Criticality: Theory, Models and Characterisation* (Cambridge University Press, Cambridge, UK, 2012).
[58] V. Buendia, S. di Santo, J. A. Bonachela, and M. A. Muñoz, Front. Phys. **8**, 333 (2020).
[59] O. Kinouchi, R. Pazzini, and Copelli, Front. Phys. **8**, 583213 (2020).
[60] V. R. V. Assis and M. Copelli, Phys. Rev. E **77**, 011923 (2008).
[61] C.-Y. Wang, Z.-X. Wu, and M. Z. Q. Chen, Phys. Rev. E **95**, 012310 (2017).
[62] J. Zierenberg, J. Wilting, V. Priesemann, and A. Levina, Phys. Rev. Research **2**, 013115 (2020).
[63] H. Bleckmann and R. Zelick, Integr. Zool. **4**, 13 (2009).
[64] P. Pichler and L. Lagnado, J. Neurosci. **39**, 112 (2019).
[65] M. Copelli, A. C. Roque, R. F. Oliveira, and O. Kinouchi, Phys. Rev. E **65**, 060901 (2002).
[66] M. Copelli, in *Cooperative Behavior in Neural Systems: Ninth Granada Lectures*, edited by J. Marro, P. L. Garrido, and J. J. Torres, AIP Conf. Proc. No. 887 (AIP, Melville, NY, 2007), p. 13.
[67] A. A. Costa, M. J. Amon, O. Sporns, and L. H. Favela, in *International Workshop on Complex Networks* (Springer, Cham, 2018), pp. 161–171.